Fate of Silica Nanoparticles in Simulated Primary Wastewater Treatment

HELEN P. JARVIE,*,† HISHAM AL-OBAIDI,‡ STEPHEN M. KING,§ MICHAEL J. BOWES,† M. JAYNE LAWRENCE,‡ ALEX F. DRAKE,‡ MARK A. GREEN,|| AND PETER J. DOBSON⊥

NERC Centre for Ecology and Hydrology, Maclean Building, Benson Lane, Crowmarsh Gifford, Wallingford OX10 8BB, U.K., Pharmaceutical Science Division, King's College London, Franklin-Wilkins Building, Stamford Street, London SE1 9NH, U.K., STFC ISIS Facility, Rutherford Appleton Laboratory, Harwell Science & Innovation Campus, Didcot OX11 0QX, U.K., Department of Physics, King's College London, Strand, London WC2R 2LS, U.K., and Department of Engineering Science, University of Oxford, Parks Road, Oxford OX1 3PJ, U.K.

Received May 11, 2009. Revised manuscript received September 3, 2009. Accepted September 4, 2009.

Through novel application of small-angle neutron scattering, we examined the fate of silica nanoparticles (SiO_2NPs) during simulated primary wastewater treatment, by measuring, in real time, the colloidal behavior of SiO_2NPs in wastewater (sewage). We examined the effects of surface functionality on SiO_2NP fate in wastewater, by comparing both unfunctionalized (uncoated or "bare") SiO_2NPs and SiO_2NPs functionalized with a thin coating of a nonionic surfactant (Tween 20), which is widely used in personal care and household product formulations containing engineered oxide nanoparticles. Our results show new evidence that the surface functionality of SiO_2NPs plays a crucial role in their flocculation and sedimentation behavior in wastewater, and thus the likely efficacy of their removal from the effluent stream during primary wastewater treatment. Uncoated SiO_2NPs did not flocculate in wastewater over typical residence times for primary treatment. Conversely, surface-functionalized (Tween-coated) SiO_2NPs underwent rapid flocculation in wastewater. Our results show that the surface-functionalized SiO_2NPs are likely to be removed by sedimentation to sewage sludge (typically recycled to land), whereas uncoated SiO_2NPs will continue through the effluent stream. While nanoparticle design is driven by use purpose, this study shows new potential for exploiting surface functionalization of nanoparticles to modify their environmental pathways.

Introduction

Nanotechnology is a multibillion dollar global industry with large increases in the production of engineered nanoparticles predicted over the next decade (*1*) and, as a result, engineered nanoparticles are being increasingly released to the environment (*2*). Engineered oxide nanoparticles (EONPs, e.g., silica (SiO_2), titania (TiO_2), ceria (CeO_2), and silver (Ag/Ag_2O)) constitute a major component of global nanomaterial production (>2 Mt y^{-1}), with a vast range of applications from ceramics, catalysts, pigments, opto-electronics, and fuel additives, to foods, cleaning and personal care products, cosmetics, and pharmaceutical formulations (*3, 4*). For a large proportion of EONPs, their major route of release into the natural environment is via sewage and industrial wastewater discharges (*5*). Wastewater treatment plants therefore act as the "gateways" controlling release of EONPs from domestic and industrial sources to aquatic or terrestrial environments: either via treated effluent which is discharged into surface waters or, via sewage sludge disposal, to land (*6*−*8*). However, there is very limited published information on the fate of EONPs during wastewater treatment (*9, 10*). Indeed, the fate of EONPs in wastewater has recently been identified as a strategic knowledge gap (*11, 12*). However, this picture is complicated by the fact that, in many of the commercial applications above, the EONPs are just one of many ingredients in the formulation. Very often surfactant and/or polymer will also be present and may (or was designed to) physically adsorb onto the surface of the EONPs (*13, 14*). In such circumstances, the interaction of the EONPs with the environment may be altered. This aspect of the environmental fate of EONPs has been little studied (*15*).

A major obstacle to investigating the environmental pathways and fate of nanoparticles is simply detecting and quantifying them in statistically significant numbers in real environmental matrices. Imaging techniques (e.g., scanning electron microscopy and atomic force microscopy) cannot be used for in situ measurements of colloidal behavior of nanoparticles in aqueous matrices and rely on per-particle analysis, which may be highly labor-intensive and only view a comparably small statistical sample set, even with modern automated optical recognition systems. Methods based on the scattering of radiation offer the fundamental advantage of direct investigation in aqueous dispersions and measurement of large statistical sample sets in comparatively short time periods. However, light scattering can be strongly perturbed by the presence of even a few larger particles and, in the case of wastewater, the background turbidity also interferes. We overcame these issues by using small-angle neutron scattering (SANS) which provides nanoparticle-selective analyses for quantifying the concentration, size, shape, and floc structure of nanoparticles within aqueous dispersions. SANS is a well-established technique applied across a wide range of disciplines, including colloid science and materials nanoscience (*16*). Although SANS has not yet been widely applied in the environmental sciences, the technique has recently been used to characterize natural aquatic nanocolloids (*17*).

Using SANS, we directly examined the colloidal behavior of synthetic silica nanoparticles (SiO_2NPs) in real wastewater matrices. We used SiO_2NPs as a "model" representative of those EONPs in widespread use because all exhibit similar surface chemistry; a surface populated by M−OH moieties (M = metal), a proportion of which are deprotonated at natural pH to give a net negative charge. SiO_2NPs have also been studied by colloid scientists for over 40 years and are

* Corresponding author phone: +44 1491 692260; fax: +44 1491 692424; e-mail: hpj@ceh.ac.uk.
† NERC Centre for Ecology and Hydrology.
‡ Pharmaceutical Science Division.
§ STFC ISIS Facility, Rutherford Appleton Laboratory.
|| Department of Physics, King's College London.
⊥ University of Oxford.

10.1021/es901399q CCC: $40.75 © 2009 American Chemical Society
Published on Web 11/15/2009

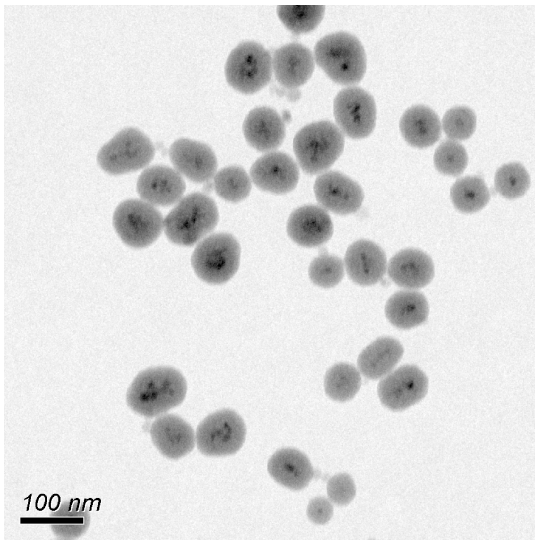

FIGURE 1. Representative transmission electron micrograph (TEM) of Fe_3O_4-cored SiO_2 nanoparticles: the darker Fe_3O_4 cores are clearly visible inside the silica shells of the nanoparticles.

widely used in household cleaning, personal care, and cosmetic products, meaning that they are routinely discharged to wastewater. Our experiment examined the partitioning of SiO_2NPs, during simulated primary (settling) treatment, between two environmental pathways: (i) nonsettleable constituents which would continue through the effluent stream, and (ii) sewage sludge which would settle out within typical residence times of ca. 2−6 h in primary settling tanks (*18*). We compared the flocculation behavior in wastewater of unfunctionalized (uncoated or "bare") SiO_2NPs and SiO_2NPs which were functionalized by adsorption of a thin coating of a nonionic surfactant, Tween 20 (also called Polysorbate 20), which is widely used in topical pharmaceutical creams, cosmetics, and domestic cleaning products. Unlike ionic surfactants, the adsorption of this class of surfactant is largely immune to nanoparticle surface charge variations.

The objective of this study was to examine the colloidal behavior of SiO_2NPs in primary wastewater treatment microcosms using small-angle neutron scattering. We examined 3 main factors controlling the colloidal stability of SiO_2NPs: (1) the composition of the aqueous matrix (by comparing wastewater and nanopure water and undertaking separate flocculation experiments in electrolyte solutions), (2) the influence of large particles which settle rapidly (by comparing raw wastewater and wastewater screened through glass wool), and (3) the effects of surface functionalization (by comparing bare and Tween-coated SiO_2NPs).

Experimental Methods

Materials. SiO_2NPs of ca. 56 nm diameter and narrow polydispersity (c. 20%), consisting of an iron (II,III) oxide core (Fe_3O_4) encapsulated in a silica (SiO_2) shell (*19*), were synthesized and characterized in-house (Figure 1; Table 1; see Supporting Information (SI) Sections 2.3 and 2.5). In terms of surface chemistry, these SiO_2NPs present at the aqueous interface like normal silica nanoparticles (the core is fully encapsulated by silica and so the iron oxide has no effect on the surface chemistry of the SiO_2NPs). Therefore, the SiO_2NPs used in this experiment will show the same colloidal behavior in wastewater as silica nanoparticles derived from commercial products. However, the presence of the Fe_3O_4 cores significantly enhances the neutron contrast of the particles, allowing the experiments to be undertaken at lower concentrations than for pure SiO_2 nanoparticles, and within the limited neutron measurement time available (see SI Sections 2.7 and 2.8). For these measurements 400 μL of aqueous nanoparticle dispersion was added to 3.6 mL of wastewater (yielding a maximum initial particle concentration of 0.09% $^{v}/_{v}$; an equivalent SiO_2NP mass concentration of 2470 mg L^{-1}). The reason for choosing this nanoparticle concentration was to produce a statistically significant scattering signal within a time frame typical of particle settling within primary treatment tanks, while ensuring that the colloidal behavior of the SiO_2NPs was not subject to interference from interparticle interactions (*17*). By analogy with our previous work (*17*), we calculate that SANS should be sensitive to concentrations of SiO_2NPs as low as ca. 100 mg L^{-1}.

Subsamples of the SiO_2NPs (0.22% $^{v}/_{v}$) were functionalized by resuspending them in a dilute solution (0.01% $^{w}/_{v}$) of the pharmaceutical-grade nonionic surfactant Tween 20 (Polysorbate 20, Figure SI-3). We calculate that, although most of the Tween molecules added to the SiO_2NPs dispersion are adsorbed (at 2−3 μmol m^{-2}), only 20−40% of the surface of the SiO_2NPs is likely to be covered in surfactant (see SI Section 5).

Raw (untreated) wastewater was sourced from the inlet stream of a wastewater treatment works serving a semiurban population of approximately 297,000 in South Central England, immediately after screening and grit removal (which excludes debris >5 mm), but before primary treatment. Background chemical characterization of the raw wastewater and information on the wastewater treatment works are supplied in the SI Sections 2.1 and 2.2 and Table SI-1). Experiments were conducted using both "raw" (untreated) wastewater and "screened" wastewater (aliquots of the same raw wastewater sample which had been passed, under gravity, through a glass wool plug, to remove larger debris and fibrous detritus, on mm length scales; Figure SI-2). Comparison of SiO_2NP settling behavior in raw and screened wastewater was undertaken to investigate the presence or absence of the larger detritus on nanoparticle sedimentation. Nanopure water (18 MΩ resistivity) was produced in-house using a Barnstead International Diamond system.

Sample Environment. Samples were sealed in 100 mm high × 2 mm path length quartz cuvettes, which were were used as a simplified and idealized settling environment (microcosm). The contents of each cuvette were fully mixed by inverting them immediately prior to the start of data collection. To comply with biological safety protocols, the sealed cuvettes were housed inside custom-built, hermetically sealed, containment vessels with neutron-transparent windows.

Small-Angle Neutron Scattering Measurements. SANS measurements were conducted on the LOQ diffractometer at the ISIS Facility (STFC Rutherford Appleton Laboratory, Oxfordshire, UK). Small-angle neutron scattering (SANS) measurements were made in nanopure water, raw and screened wastewater, both before and after dosing with unfunctionalized and Tween-coated SiO_2NPs. Measurements were taken alternately at each of two vertical positions within the aqueous phase along a cuvette (the lower measurement position was located just above any sedimented material), at approximately 30 min intervals over a period of up to 3−6 h. Data were recorded on two, two-dimensional, position-sensitive detectors spanning different ranges of scattering angle 2θ, but which overlapped in Q-space, where the angular scattering vector, Q:

$$Q = \frac{4 \cdot \pi \cdot \sin(\theta)}{\lambda} \quad (1)$$

and λ is the neutron wavelength.

Data Analysis. Raw scattering data were corrected for the experimentally determined neutron transmission and known path length of each sample, and for the efficiency of the

TABLE 1. Summary of SANS Data (See SI Section 2.9 for an Explanation of the Analyses Used)[a]

sample	position	elapsed	polydisperse spheres				surface fractals			[SiO_2NP]
		(hh:mm)	$n \pm 0.01$	Φ_{eff} (%v/v) $\pm$ 0.001	d (nm) $\pm$ 0.4	PD (%) $\pm$ 1	Φ_{eff} (%v/v) $\pm$ 0.001	$D_s \pm 0.01$	$D_m \pm 0.01$	(mg L^{-1}) $\pm$ 200
nanopure water + SiO_2NP	T & B	03:07	4.70	0.015	56.0	22	0.047	2.73	3.71	2470[c]
nanopure Water + Tween-SiO_2NP[b]	T & B	06:36	4.65	0.019	61.4	20	0.077	2.73	3.69	2470[c]
raw wastewater + SiO_2NP	T	03:15	4.63	0.015	54.2	21	0.050	2.73	3.68	2628
raw wastewater + SiO_2NP	B	03:36	4.47	0.014	52.4	20	0.052	2.74	3.61	2733
screened wastewater + SiO_2NP	T	03:13	4.74	0.013	56.0	18	0.054	2.74	3.74	2838
screened wastewater + SiO_2NP	B	03:35	4.51	0.014	53.2	20	0.048	2.74	3.63	2522
SiO_2NP mean $\pm$ 1 standard deviation					54.4 $\pm$ 1.6	20 $\pm$ 2		2.74 $\pm$ 0.01		
raw wastewater + Tween-SiO_2NP	T	00:34	4.08	0.007	55.2	20	0.022	2.74	3.41	706
raw wastewater + Tween-SiO_2NP	T	01:25	4.19	0.004	58.7	17	0.019	2.74	3.46	609
raw wastewater + Tween-SiO_2NP	B	01:03	4.33	0.005	52.8	24	0.015	2.73	3.53	481
raw wastewater + Tween-SiO_2NP	B	02:12	4.33	0.004	54.5	20	0.011	2.69	3.51	353
screened wastewater + Tween-SiO_2NP	T	00:39	4.19	0.004	57.2	20	0.017	2.74	3.47	545
screened wastewater + Tween-SiO_2NP	T	01:30	4.15	0.002	56.1	20	0.001	2.53	3.34	32
screened wastewater + Tween-SiO_2NP	B	01:08	4.14	0.003	55.1	18	0.005	2.66	3.40	160
screened wastewater + Tween-SiO_2NP	B	01:51	4.00	0.003	47.2	27	0.007	2.74	3.37	224
Tween-SiO_2NP mean $\pm$ 1 standard deviation					55.3 $\pm$ 4.0	21 $\pm$ 3		2.70 $\pm$ 0.07		

[a] T & B refer to the top and bottom measuring positions in the cuvette, the centers of which were 63 mm apart. The elapsed time is given to the end of data collection at the position specified. Model parameters: $-n$ is the Q dependence of the SANS data at $Q < 0.2$ nm^{-1}, Φ_{eff} is the effective particle volume fraction, d is the effective particle diameter, PD is the Schultz polydispersity defined as $2\sigma/\langle d \rangle$ where σ is the rms deviation on the mean size, D_s is the surface fractal dimension, and D_m is the resulting mass fractal dimension (see SI Section 2.9). The SiO_2NP concentration is calculated from the surface fractal Φ_{eff} as explained in the main text. The same background level was used across all model fits on a given sample. [b] When modeled as a core+shell nanoparticle the effective diameter is 68 nm; 2 $\times$ (29.5 + 4.5) nm. [c] Dosing concentration.

TABLE 2. Summary of Supplementary Tests of SiO_2NP Colloidal Stability in Electrolyte Solutions

nanoparticle type	electrolyte solution	observations
unfunctionalized (uncoated) SiO_2NP	0.01 M $La(NO_3)_3$	rapid and significant flocculation within 8 min; complete flocculation after 30 min
	0.10 M $La(NO_3)_3$	slow flocculation over the first 30 min but incomplete
functionalized (Tween-coated) SiO_2NP	0.01 M NaCl	no effect after 72 h
	0.01 M $La(NO_3)_3$	no effect in first 5 min; slow flocculation over the next hour; complete flocculation after 2 h
	0.10 M $La(NO_3)_3$	no effect in first 5 min; slow flocculation over the next hour; complete flocculation after 2 h

detectors, according to standard procedures using the instrument-specific software, before being converted into "scattered neutron intensity" data as a function of Q, $I(Q)$. Changes in the SANS intensity $I(Q)$ were used to monitor changes in SiO_2NP concentrations and particle size. The angular variation in $I(Q)$ from a two-phase sample may be written in a very general form as

$$I(Q) = K \cdot \phi_1 \cdot \phi_2 \cdot (\rho_1 - \rho_2)^2 \cdot F(Q) + B \qquad (2)$$

where K is a calibration factor (e.g., converting the data to absolute intensities), and ϕ_i is the volume fraction ($\phi_1 + \phi_2 = 1$) and ρ_i is the neutron scattering length density (see SI Section 2.8), of phase i. The term in brackets—known as the "contrast"—describes the relative "visibility" of the phases, while $F(Q)$—known as the "scattering law"—describes how the scattering is modulated by size, shape, and local order. B is the residual background signal.

Nanoparticle diameter (d), polydispersity, effective nanoparticle volume fraction (i.e., nanoparticle "concentration"; Φ_{eff}), surface fractal dimension (D_s), and mass fractal dimension (D_m) were then derived by fitting the scattering data to established scattering laws for polydisperse homogeneous spheres and for surface fractals (see SI Section 2.9).

Further details may be found in the Supporting Information on the nanoparticle synthesis (Section 2.3), functionalization (Section 2.4), characterization (including particle size) (Section 2.5), sample containment (Section 2.6), and technical details of the neutron beamline and the data reduction and modeling procedures (Sections 2.7 and 2.9).

Supplementary Tests of SiO_2NP Colloidal Stability in Electrolyte Solutions. At the pH of the wastewater (7.18) the unfunctionalized silica surface carries a net negative charge. If the adsorbed surfactant layer were incomplete then both the functionalized *and* unfunctionalized SiO_2NPs should be susceptible to the presence of added electrolyte (cations). To test this, aliquots of both types of SiO_2NPs dispersion were mixed 1:1 with 0.02 and 0.20 M solutions of the classic colloidal coagulant $La(NO_3)_3$ in nanopure water, (Figures SI-6 and SI-7 and Table 2). These electrolyte concentrations were chosen to equal, and exceed by an order of magnitude, the known maximum electrolyte concentrations the nanoparticles would have been exposed to in the wastewater. However, according to the Schulze–Hardy rule, a M^{3+} counterion should be 1000 times more effective as a coagulant than a M^{1+} counterion (e.g., Na).

Results and Discussion

SANS Characterization of Wastewater, SiO_2NP Dispersions, and the Adsorbed Surfactant Layer. The SANS data (plotted in Figure 2 as intensity, $I(Q)$, versus the angular vector, Q) from nanopure water, raw wastewater, and screened wastewater are near-flat lines, showing that, in the absence of SiO_2NPs, nothing in the raw or screened wastewater contributes any background neutron scattering beyond that from nanopure water alone. In contrast, strong scattering was observed when each matrix was dosed with unfunctionalized (uncoated) SiO_2NPs or functionalized (Tween-coated) SiO_2NPs. Unfunctionalized SiO_2NPs in nanopure water could be successfully modeled as a dispersion of polydisperse, noninteracting, homogeneous spheres of ca. 56 nm diameter. This particle size is consistent with our supporting measurements derived from TEM and light scattering (see SI Section 2.5). Although the nanoparticle dosing concentration is still some 10,000 times higher than might currently be expected for nanoparticle concentrations in wastewater (based on published estimates *4*, *20*), in all cases the SANS data could be adequately modeled without invoking an additional interparticle pair potential contribution. This means that, at the concentrations studied, interparticle interactions are so long-range and so weak that they can be reasonably ignored. In addition, the absence of any features in the SANS data that could be due to an interparticle structure factor, $S(Q)$ (see SI Section 2.9 and Figure SI-12) provides further conclusive proof that the environmentally high nanoparticle concentration in this experiment ($0.09\%^{v}/_{v}$) does not have any implication for the flocculation and settling behavior of these SiO_2NPs in wastewater. Indeed, our findings support previous work on natural aquatic nanoparticles, which showed that interparticle interactions are negligible at concentrations <3% $^{v}/_{v}$ (*17*).

From the SANS data (Table 1), the thickness of the adsorbed surfactant layer functionalizing the SiO_2NPs was estimated to be between 2.5 and 4.5 nm (depending on the analysis), which is consistent with the calculations of surfactant adsorbed amount (see SI Section 5).

Colloidal Stability of SiO_2NPs in Nanopure Water. In nanopure water, both the unfunctionalized SiO_2NPs and Tween-coated SiO_2NPs were stable throughout the SANS experiment (ca. 3–6 h), and visual observations confirmed that stability continued at >24 h after dosing (Figure SI-5). The calculated Stokes settling velocity for 60 nm spheres of density 2.8 g cm^{-3} (cf 2.2 g cm^{-3} for normal silica) in water is just 0.3 mm per day (see SI eq SI-10, Section 4); therefore, only flocculation will remove these SiO_2NPs from the water column over the relevant retention times in primary settling tanks.

Using the spherical scattering model, the effective particle volume fraction, Φ_{eff}, in nanopure water (Table 1) is only about 20% of the known particle volume fraction on dosing ($0.09\%^{v}/_{v}$). This underestimation is likely to be a result of the nonuniform composition of the SiO_2NPs and their imperfectly spherical shape (as shown by TEM and some SANS analyses using models for monodisperse ellipsoids of revolution, the latter suggesting axial ratios close to 1:1:2). However, the unusually high value of the power law exponent describing the angular variation of the scattering, n (>4), related to the fractal dimensions characterizing the system (see SI Section 2.9), also shows that the interface between the SiO_2NPs and the aqueous matrix is rather diffuse and that SiO_2NPs show surface fractal properties (*21*). Indeed, a much better agreement between Φ_{eff} and the dosed concentration (within 50%)

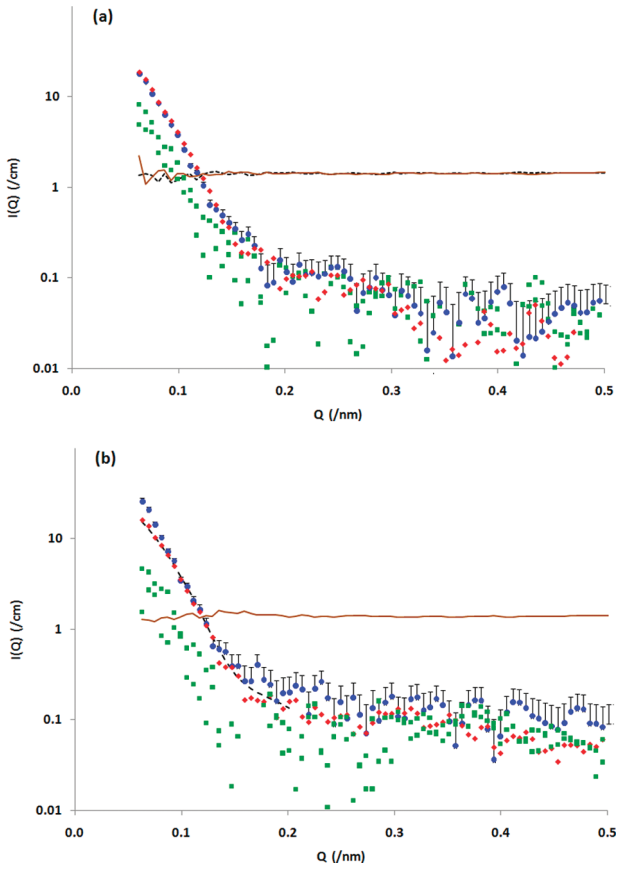

FIGURE 2. (a) Small-angle neutron scattering data from unfunctionalized and Tween-coated Fe_3O_4-cored silica nanoparticles (SiO_2NPs) in *raw* wastewater and nanopure water (in the absence of added electrolyte). Key: (circles) nanopure water + unfunctionalized SiO_2NPs (2 h); (diamonds) *raw* wastewater + unfunctionalized SiO_2NPs (2 h); (squares) *raw* wastewater + Tween-coated SiO_2NPs (30 and 90 min); (dashed line) nanopure water; and (continuous line) *raw* wastewater alone (both lines are displaced for clarity by 1/cm). All data were collected at the top measurement position (68 mm above the bottom of the sample cuvette), after the times indicated, with the background scattering from the respective aqueous matrices subtracted from the SiO_2NP data. Where shown, error bars depict the measured standard deviation and are representative of those for all samples. (b) Small-angle neutron scattering data from unfunctionalized and Tween-coated Fe_3O_4-cored SiO_2NPs in screened wastewater, and from Tween-coated SiO_2NPs in nanopure water (in the absence of added electrolyte). Key: (circles) nanopure water + Tween-coated SiO_2NPs (2 h); (diamonds) *screened* wastewater + unfunctionalized SiO_2NPs (2 h; (squares) *screened* wastewater + Tween-coated SiO_2NPs (30 and 90 min); (continuous line) *screened* wastewater alone; and (dashed line) model fit for 53 nm diameter spheres. Conditions same as for (a).

is obtained with the surface fractal model which interprets the SiO_2NPs as discrete but irregular objects. This model shows that, in nanopure water, SiO_2NPs behave as surface fractals of dimension $D_s = 2.7$, supporting the inference that the interface between the surface of the SiO_2NPs and the aqueous matrix is diffuse. A likely explanation is that the silica shell of these SiO_2NPs is actually quite porous (i.e., has a low degree of cross-linking). The surface fractal model was therefore used for quantifying SiO_2NPs concentrations in the remainder of this work. The higher Φ_{eff} for the Tween-coated NPs (given the same original SiO_2NPs mass concentration) reflects the presence of the adsorbed surfactant layer.

By equating the fractal model-derived Φ_{eff} values in nanopure water, for both unfunctionalized SiO_2NPs and Tween-coated SiO_2NPs, with the dosed concentration and then assuming a linear relationship, mass concentrations can be calculated for each SANS data set. This provides a direct mass-based quantification of SiO_2NP removal by sedimentation. The values obtained are shown in Table 1.

Colloidal Stability of SiO_2NPs in Wastewater. As in nanopure water, unfunctionalized SiO_2NPs were also completely stable in both raw and screened wastewater, with mass concentrations (within analytical error) very similar to the as-dosed SiO_2NP concentration (2470 mg/L). This demonstrates that no sedimentation occurred over a period of around 3 h (visual observations confirmed that this stability continued at ca. 24 h after dosing). This shows that no interactions between unfunctionalized SiO_2NPs and wastewater constituents induced SiO_2NP flocculation within time scales typical of wastewater transit through the sewerage network (*22*) and within primary treatment. Unfunctionalized SiO_2NPs are therefore likely to pass straight through primary wastewater treatment and continue in the effluent stream.

While Tween-coated SiO_2NPs were completely stable in nanopure water over 24 h, they were much *less* stable in both raw and screened wastewater. Immediately following dosing with Tween-coated SiO_2NPs, rapid sedimentation of the nanoparticles and sewage particulates was visually observed over a few seconds, although a pale yellow color remained to the dispersion, indicating that some Tween-coated SiO_2NPs were retained in suspension a few minutes later. The SANS data from Tween-coated SiO_2NPs in raw and screened wastewater were noticeably less intense (Figure 2) and, after 90 min $I(Q \rightarrow 0)$ was as much as an order of magnitude lower than comparable data for the unfunctionalized SiO_2NPs in wastewater. The loss of intensity results from reductions in concentrations of the Tween-coated SiO_2NPs of up to 90% (Table 1), evidence of a dramatic flocculation of the Tween-coated SiO_2NPs in wastewater within 90 min. Despite this, it was still possible to detect the presence of Tween-coated SiO_2NPs at both measurement positions after 2 h. Indeed, their particle sizes in suspension after 2 h were very similar to those measured at shorter time scales and also similar to the particle sizes of the unfunctionalized SiO_2NPs. This indicates that those Tween-coated SiO_2NPs remaining in suspension were unaggregated. In contrast, unfunctionalized SiO_2NPs remained in a stable colloidal dispersion in wastewater throughout the experiment.

Quantifying SiO_2NP Sedimentation from SANS Data. Sedimentation losses of Tween-coated SiO_2NPs in wastewater can be quantified by the change in concentration, relative to the initially dosed concentration, over the measurement period (Table 1). At the upper measurement position, 71−78% mass loss of Tween-coated SiO_2NPs occurred after 0.5−0.7 h; after 1.5 h, almost complete loss (99%) occurred in screened wastewater, compared with 75% loss in the raw wastewater. At the lower measurement position, corresponding losses of Tween-coated SiO_2NPs were 81−94% after 1.1 h and 86−91% after 1.9−2.2 h. These sedimentation losses exceed any fluctuations in concentration which may result from analytical error (<10%). There is some evidence to suggest that the sedimentation losses at both measurement positions were slightly higher in the screened wastewater than in the raw wastewater. This may indicate that, in the raw wastewater, the very small proportion of larger detrital particulates or fibers, which bridge the walls of the cuvette, may partially retard the sedimentation of the Tween-coated SiO_2NPs. However, if the nanoparticles were attractively interacting with this suspended detrital material, much higher sedimentation rates would be expected in the raw wastewater. This is because the vast majority of the detrital material settles out very rapidly. The fact that we see a slightly higher sedimentation rate in screened sewage is therefore evidence

that the presence of suspended detrital material is of minor significance for SiO_2NP sedimentation.

Assuming the sedimentation rate is constant, settling velocities, v_s, can be estimated. Thus for Tween-coated SiO_2NPs in screened wastewater at the lower measurement position, 94% removal to a depth of 100 mm in 1.13 h yields $v_s \approx 83$ mm h^{-1}. However, this is likely to be a vast underestimate of the actual settling velocities of these SiO_2NPs which were observed to undergo rapid settling immediately after dosing. Visual observations suggest that for some particles v_s is likely to be at least an order of magnitude higher (>1000 mm h^{-1}), although neither this, nor the proportion of Tween-coated SiO_2NPs with these higher settling velocities, could be directly quantified in the current experiment. That would be technically feasible but would require more intensive time-resolved measurements.

Wastewater primary sedimentation studies indicate that settleable particles typically have v_s >360 mm h^{-1} (*23*). Our visual observations, along with the large reductions in mass concentrations (for typical primary treatment retention times), therefore suggest that the flocculation of Tween-coated SiO_2NPs in wastewater will produce agglomerates which have the potential to settle out during primary treatment and thus be removed from the effluent stream and get incorporated into the sewage sludge. We acknowledge that full-scale primary clarifier settling characteristics may not be as efficient as the microcosms used in this experiment; however, in this experiment, we focus on understanding the factors influencing the colloidal stability of SiO_2NPs in wastewater. Further work will be required to establish the impacts of the more complex hydrodynamics in full-scale primary settling tanks on SiO_2NP settling.

Role of Electrolytes in the Colloidal Stability of SiO_2NPs in Wastewater. To further explore the stability of the SiO_2NPs, 0.01 M $La(NO_3)_3$ (the effective electrolyte concentration of the wastewater was equivalent to 0.01 M NaCl) was added to both unfunctionalized and Tween-coated SiO_2NPs in nanopure water (Table 2). Very rapid flocculation of the unfunctionalized SiO_2NPs was observed in 0.01 M $La(NO_3)_3$ because the silica shell is negatively charged at natural pH. The slower flocculation of the unfunctionalized nanoparticles by the stronger electrolyte is believed to be the result of effective charge reversal in the electrical double layer leading to a degree of colloidal restabilization.

However, the time scales of electrolyte-induced flocculation of the Tween-coated SiO_2NPs were considerably longer (1−2 h). The gradual flocculation of Tween-coated SiO_2NPs in electrolyte solution, compared with the immediate and rapid flocculation of unfunctionalized SiO_2NPs in the same matrix, confirms the presence of an incomplete adsorbed layer of surfactant. This demonstrates that the rapid flocculation of Tween-coated SiO_2NPs in wastewater is *not* an electrolyte effect and must instead be mediated by interactions between the adsorbed Tween molecules and other constituents of sewage (raw sewage solids are predominantly organic matter (*24*), derived largely from household wastes and feces, and composed of a complex mixture of fats, proteins, amino acids, sugars, cellulose, humic substances, and micro-organisms (*25*)). Conversely, the long-term (>24 h) stability of unfunctionalized SiO_2NPs in raw and screened wastewater demonstrates that the sewage organic matter did not bring about aggregation of the unfunctionalized SiO_2NPs. Indeed, at electrolyte concentrations in nanopure water equivalent to those present in wastewater, flocculation of unfunctionalized SiO_2NPs occurred within 30 min. This means that the interaction of unfunctionalized SiO_2NPs with other (nonelectrolyte) wastewater constituents, such as sewage organic matter, promotes this longer-term colloidal stability.

Our results therefore suggest that Tween-coated SiO_2NPs in wastewater may undergo two modes of flocculation, which occur simultaneously but over differing time scales: (i) rapid flocculation mediated by interactions between adsorbed Tween molecules and sewage organic matter, and (ii) a slower electrolyte-mediated flocculation process

Implications of Surface Functionalization for Sedimentation Behavior of SiO_2NPs in Wastewater. By modifying the surface functionality of SiO_2NPs we have shown a dramatic difference in their colloidal behavior and fate in wastewater. Our results show that unfunctionalized SiO_2NPs are stable and unsettlable in wastewater over typical time scales of transit through the sewerage network and during the primary wastewater treatment process, indicating that they will pass directly to the secondary treatment stage. In contrast, SiO_2NPs functionalized with a nonionic surfactant readily undergo flocculation on the same time scales and are likely to be retained by primary sedimentation. Our results suggest that functionalized (Tween-coated) SiO_2NPs will pass along a different environmental pathway, via sewage sludge, which is used as an agricultural fertilizer, is disposed of to landfill, or is used in land reclamation. In the UK at present, it is estimated that approximinately 60% of treated sludge is reused in farming as a fertilizer (*26*).

Further work is now needed to test the wider applicability of these results to a wider range of EONPs, surfactants, and wastewaters. Our experiments were undertaken using wastewater which is representative of typical domestic wastewater composition (see Table SI-1). However, it is possible that differences in composition of wastewaters from different sources (particularly those receiving industrial effluents) may have an impact on the stability/flocculation rates of nanoparticles and further work is needed to explore these effects. Microbes may also use the Tween as a food source and further work is needed to establish whether microbial action might remove the surfactant coating, with potential implications for the passage of nanoparticles through the wastewater treatment plant.

Further time-resolved studies are also needed to quantify the differences in settling velocities as a result of interactions with other wastewater constituents (e.g., sewage organic matter) and electrolyte-induced agglomeration, and the implications for rates of SiO_2NP removal by primary sedimentation. It would also be valuable to examine the effects of varying surfactant surface coverage on nanoparticle flocculation behavior.

Here, we provide a first assessment of how primary wastewater treatment may vary in its efficiency to remove SiO_2NPs with different surface functionality. These findings have wider implications for the potential exposure of microbial flocs and biofilms in secondary treatment processes to engineered oxide nanoparticles. This is of strategic importance because some recent studies have indicated that these microbial communities may be compromised by exposure to oxide nanoparticles, with potential consequences for the overall efficiency of wastewater treatment works (*27*, *28*). We have used SANS to examine the fate of SiO_2NPs in real wastewater matrices by quantifying changes in their concentrations in response to flocculation and sedimentation. Indeed, these measurements could not have been made using conventional light scattering or microscopy techniques. This work demonstrates the considerable future potential for SANS in environmental fate and behavior studies of nanoparticles in natural waters (e.g., riverine, groundwater, estuarine, and marine environments) as well as wastewaters and effluents. While nanoparticle design is driven by use purpose, our results offer an exciting prospect that, by manipulating the surface functionality of EONPs, it may be possible to optimize or direct their fate along particular environmental pathways, with wide-ranging implications for

the environmental management of wastes from nanotechnology industries and their consumer products.

Acknowledgments

H.P.J. and S.M.K. are joint first authors. We thank S. Waller and B. Holsman for the design of the Biological Containment Vessels; the ISIS Facility for funding construction of the vessels and providing neutron beam time; Anglian Water Services for granting access to the treatment works; and J. Penfold for useful discussions. This work was funded by the UK Natural Environment Research Council under the Environmental Nanoscience Initiative (grant NE/E014585/1).

Supporting Information Available

Details of SiO_2NP synthesis, functionalization, characterization, and the assessment of colloidal stability, together with details of SANS measurements and the scattering functions used to analyze the data. This material is available free of charge via the Internet at http://pubs.acs.org.

Literature Cited

(1) *Novel Materials in the Environment: The Case of Nanotechnology*; UK Royal Commission on Environmental Pollution, 2008.

(2) *Characterising the Potential Risks Posed by Engineered Nanoparticles: A Second UK Government Research Report*; UK Department of the Environment Food and Rural Affairs, 2007.

(3) Ju-Nam, Y.; Lead, J. R. Manufactured nanoparticles: an overview of their chemistry, interactions and potential environmental implications. *Sci. Total Environ.* **2008**, *400*, 396–414.

(4) Boxall, A. B. A., Chaudry, Q., Sinclair, C., Jones, A., Aitken, R. J., Jefferson, B., Watts, C. *Current and Predicted Environmental Exposure to Engineered Nanoparticles*; Central Science Laboratory, UK Department of the Environment Food and Rural Affairs, 2007.

(5) Boxall, A. B. A.; Tiede, K.; Chaudry, Q. Engineered nanomaterials in soils and water: how do they behave and could they pose a risk to human health? *Nanomedicine* **2007**, *2* (6), 919–927.

(6) Colvin, V. L. The potential environmental impact of engineered nanomaterials. *Nat. Biotechnol.* **2003**, *21*, 1166–1170.

(7) Wiesner, M. R.; Lowry, G. V.; Alvarez, P.; Dionysiou, D.; Biswas, P. Assessing the risks of manufactured nanomaterials. *Environ. Sci. Technol.* **2006**, *40* (14), 4336–4345.

(8) Evans, J. Small but scary? *Chem. World* **2006**, *3* (11), 58–62.

(9) Chang, M. R.; Lee, D. J.; Lai, J. Y. Nanoparticles in wastewater from a science-based industrial park - coagulation using polyaluminum chloride. *J. Env. Manange.* **2007**, *85*, 1009–1014.

(10) Limbach, L. K.; Bereiter, R.; Mueller, E.; Krebs, R.; Gaelli, R.; Stark, W. J. Removal of oxide nanoparticles in a model wastewater treatment plant: Influence of agglomeration and surfactants on clearing efficiency. *Environ. Sci. Technol.* **2008**, *42*, 5828–5833.

(11) *Nanotechnology White Paper*; 100/B-07/001; U.S. Environmental Protection Agency: Washington, DC, 2007.

(12) Scheringer, M. Nanoecotoxicology - Environmental risks of nanomaterials. *Nat. Nanotechnol.* **2008**, *3*, 322–323.

(13) Fleer, G. J., Cohen Stuart, M. A., Scheutjens J. M. H. M., Cosgrove, T., Vincent, B., Eds. *Polymers at Interfaces*; Chapman & Hall: London, 1993.

(14) Papirer, E., Ed. *Adsorption on Silica Surfaces*; Surfactant Science Series 90; Marcel Dekker Inc: New York, 2000.

(15) Nowack, B.; Bucheli, T. D. Occurrence, behavior and effects of nanoparticles in the environment. *Environ. Pollut.* **2007**, *150* (1), 5–22.

(16) King, S. M. Small angle neutron scattering. In *Modern Techniques for Polymer Characterisation*; Pethrick, R. A., Dawkins, J. V., Eds.; John Wiley & Sons: New York, 1999.

(17) Jarvie, H. P.; King, S. M. Small-angle neutron scattering study of natural aquatic nanocolloids. *Environ. Sci. Technol.* **2007**, *41*, 2868–2873; and accompanying Supporting Information.

(18) Waites M. J., Morgan, N. L., Rockey, J. S., Higton, G. *Industrial Microbiology: An Introduction.*; Blackwell Publishing, 2001.

(19) Bumb, A.; Brechbiel, M. W.; Choyke, P. L.; Fugger, L.; Eggeman, A.; Prabhakaran, D.; Hutchinson, J.; Dobson, P. J. Synthesis and characterization of ultra-small superparamagnetic iron oxide nanoparticles thinly coated with silica. *Nanotechnology* **2008**, *19*, 335601.

(20) Mueller, N. C.; Nowack, B. Exposure modeling of engineered nanoparticles in the environment. *Environ. Sci. Technol.* **2008**, *42*, 4447–4453.

(21) Schmidt, P. W.; Avnir, D.; Levy, D.; Hohr, A.; Steiner, M.; Roll, A. Small-angle x-ray scattering from the surfaces of reversed-phase silicas: Power-law scattering exponents of magnitudes greater than four. *J. Chem. Phys.* **1991**, *94*, 1474–1479.

(22) Holt, M. S.; Fox, K. K.; Burford, M.; Daniel, M.; Buckland, H. UK monitoring study on the removal of linear alkylbenzene sulphonate in trickling filter type sewage treatment plants. Contribution to GREAT-ER project #2. *Sci. Total Environ.* **1998**, *210* (1−6), 255–269.

(23) Andoh, R. Y. G.; Smisson, R. P. M. The practical use of wastewater characterisation in design. *Water Sci. Technol.* **1996**, *33* (9), 127–134.

(24) *Sewage Works and Sewage Farms*; ISBN 1 85112 282 6; Department of the Environment Industry Profile (Contaminated Land Research Programme), 1995.

(25) Czechowski, F.; Marcinkowski, T. Sewage sludge stabilisation with calcium hydroxide: effect on physicochemical properties and molecular composition. *Water Res.* **2006**, *40*, 1895–1905.

(26) Bruce, A. M., Evans, T. D. Sewage sludge disposal: Operational and environmental issues. Review of Current Knowledge; FR/R0001; Foundation for Water Research, 2002.

(27) Choi, O.; Deng, K. K.; Kim, N. J.; Ross, L.; Surampalli, R. Y.; Hu, Z. The inhibitory effects of silver nanoparticles, silver ions and silver chloride colloids on microbial growth. *Water Res.* **2008**, *42* (12), 3066–3074.

(28) Neal, A. L. What can be inferred from bacterium-nanoparticle interactions about the potential consequences of environmental exposure to nanoparticles? *Ecotoxicology* **2008**, *17*, 362–371.

ES901399Q